Journal of Organometallic Chemistry, 372 (1989) 417–435
Elsevier Sequoia S.A., Lausanne – Printed in The Netherlands
JOM 20039

Reaction of Ph_2PH with the tetracobalt cluster $Co_4(CO)_{10}(\mu_4\text{-}PPh)_2$. Kinetic studies of sequential CO replacement and X-ray crystal structure of $Co_4(CO)_8(\mu_4\text{-}PPh)_2(Ph_2PH)_2$

Ming-Jaw Don, Michael G. Richmond *

Center for Organometallic Research and Education, Department of Chemistry, University of North Texas, Denton, TX 76203 (U.S.A.)

William H. Watson * and Ante Nagl **

Department of Chemistry, Texas Christian University, Forth Worth, TX 76129 (U.S.A.)

(Received February 27th, 1989)

Abstract

The kinetics for the sequential substitution of CO on the tetracobalt cluster $Co_4(CO)_{10}(\mu_4\text{-}PPh)_2$ have been investigated for the ligand Ph_2PH. Ligand substitution is observed under mild conditions to yield $Co_4(CO)_{10-n}(\mu_4\text{-}PPh)_2(Ph_2PH)_n$ ($n = 1, 2$). The kinetics for each substitution step reveal a two-term rate law: $(k_1 + k_2[Ph_2PH])[\text{cluster}]$. The k_2 component corresponds to a Ph_2PH-dependent attack on $Co_4(CO)_{10}(\mu_4\text{-}PPh)_2$ and $Co_4(CO)_9(\mu_4\text{-}PPh)_2(Ph_2PH)$. The k_1 contribution is inconsistent with a dissociative loss of CO, but rather a unimolecular *closo* → *nido* cluster rearrangement. The bis-substituted cluster $Co_4(CO)_8(\mu_4\text{-}PPh)_2(Ph_2PH)_2$ is observed to crystallize in the triclinic space group $P\bar{1}$ with a 9.800(1) Å, b 14.849(2) Å, c 15.583(2) Å, α 83.89(1)°, β 81.69(1)°, γ 79.34(1)°, V 2197.7(5) Å^3 and $Z = 2$. Block-cascade least-squares refinement yielded $R = 0.0379$ for 4860 reflections. The importance of thermodynamic product control in directing the phosphine regiochemistry and stereochemistry in $Co_4(CO)_8(\mu_4\text{-}PPh)_2(Ph_2PH)_2$ and other reported clusters of this genre is discussed.

Introduction

Ligand substitution reactions in polynuclear metal clusters continue to receive wide attention in many laboratories [1–16]. Electronic and/or steric directing effects originating from adjacent metal centers have been shown to influence the

---

* Authors to whom correspondence should be addressed.

** Present address: Faculty of Technology, University of Zagreb, Zagreb (Yugoslavia).

0022-328X/89/$03.50

rate of dissociative CO loss and to assist in determining the regiochemistry and stereochemistry of the incoming ligand about the cluster polyhedron [17–29]. Examples of substitution reactions arising from reversible metal–metal bond scission (homolytic or heterolytic) have also been reported [30–39]. Here the act of bond scission leads to a coordinatively unsaturated cluster that may undergo reaction in the presence of ligand. Recently, careful kinetic studies by Huttner et al. have provided compelling data for the involvement of such reactive intermediates [40]. Finally, the redox activation of clusters in substitution reactions has been gaining increased attention [41–48]. These odd-electron multinuclear complexes are typically several orders of magnitude more reactive than the corresponding neutral cluster, behavior that parallels the many reported examples of enhanced substitutional reactivity in paramagnetic mononuclear complexes [49].

Our interest in the tetracobalt cluster $Co_4(CO)_{10}(\mu_4\text{-}PPh)_2$ and its phosphinated derivatives stems from their reported catalytic activity in the hydroformylation of 1-pentene [50] along with the varied regiochemistry and stereochemistry attendant upon ligand substitution [51–53]. A detailed study of the substitutional reactivity of $Co_4(CO)_{10}(\mu_4\text{-}PPh)_2$ with $P(OMe)_3$ has been previously reported [55]. Thermal ligand substitution was observed to afford mono, bis, tris, and tetrakis derivatives under mild conditions. Interestingly enough, reaction to give mono- and bis-substituted derivatives occurred via a two-term rate law where rate = $(k_1 + k_2[P(OMe)_3])[\text{cluster}]$. Furthermore, it was suggested that the k_1 term represented a unimolecular cluster rearrangement that was independent of CO loss or phosphite attack. In order to test the generality of the earlier rate law for mono- and bis-substitution and to further investigate the possible intervention of a Co–Co bond scission process, we studied the substitution kinetics using the larger phosphine ligand Ph_2PH. We report our results herein.

Results

Substitution kinetics

The reaction of Ph_2PH with $Co_4(CO)_{10}(\mu_4\text{-}PPh)_2$ (**1**) (eq. 1) followed pseudo-first-order kinetics for a minimum of three half-lives over the temperature range between 20 and 40 °C. Figure 1 shows the infrared spectral changes for a typical reaction that leads to the production of the mono-substituted cluster $Co_4(CO)_9(\mu_4\text{-}PPh)_2(Ph_2PH)$ (**2**). Clearly visible are the isosbestic points at 2051, 2025, 2017, 2008 and 1862 cm^{-1} which confirm the substitution reaction as an equilibrium system. Table 1 gives the pseudo-first-order rate constants (k_{obsd}) obtained under the listed reaction conditions. A plot of the various k_{obsd} values as a function of Ph_2PH concentration is shown in Fig. 2, from which the ligand-independent and ligand-dependent rate constants k_1 and k_2, respectively, are readily obtained (Table 2).

$$\underset{(\mathbf{1})}{Co_4(CO)_{10}(\mu_4\text{-}PPh)_2} + Ph_2PH \rightarrow \underset{(\mathbf{2})}{Co_4(CO)_9(\mu_4\text{-}PPh)_2(Ph_2PH)} + CO \qquad (1)$$

The effect of tri-n-butyltin hydride on the substitution rate k_{obsd} was next examined because $Co_4(CO)_{10}(\mu_4\text{-}PPh)_2$ is known to undergo facile electron-transfer-chain (ETC) catalyzed ligand substitution [41,56*]. This additive was chosen

---

* Reference number with asterisk indicates a note in the list of references.

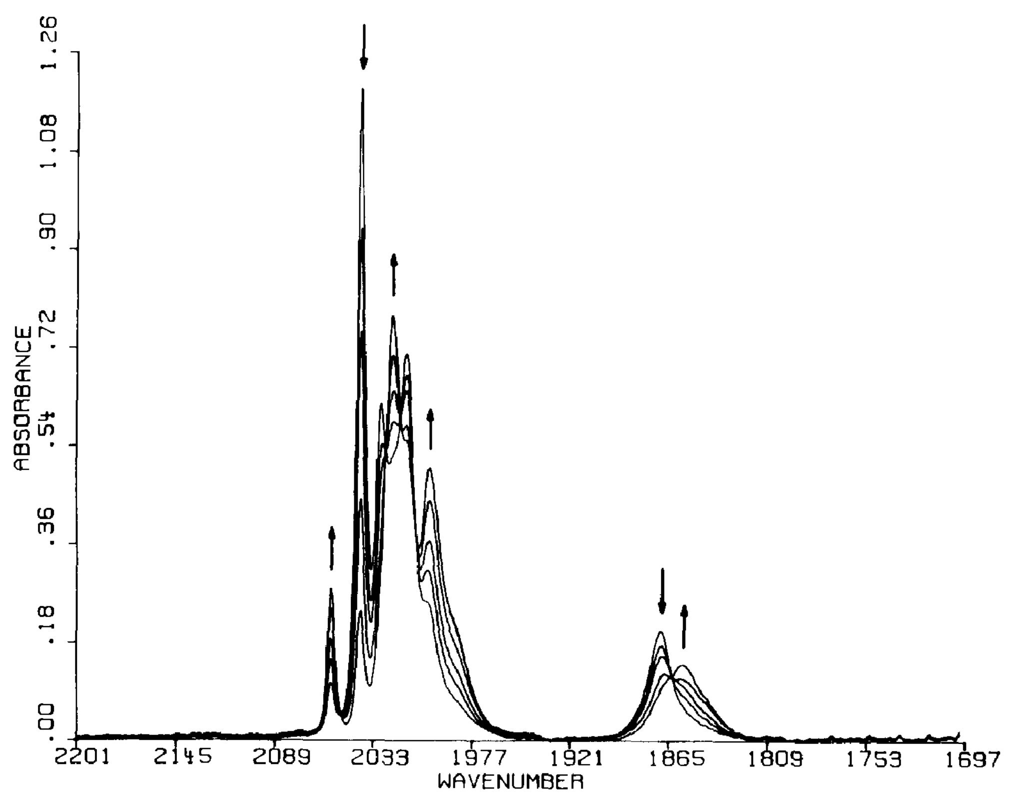

Fig. 1. Typical infrared spectral changes accompanying the ligand substitution of $Co_4(CO)_{10}(\mu_4\text{-PPh})_2$ (**1**) with Ph_2PH to afford $Co_4(CO)_9(\mu_4\text{-PPh})_2(Ph_2PH)$ (**2**).

due to its ability to function as an efficient inhibitor of free-radical-chain processes involving metal carbonyls [57]. Furthermore, tri-n-butyltin hydride effectively terminates the ETC catalyzed substitution pathway in $Co_4(CO)_{10}(\mu_4\text{-PPh})_2$ [41]. Since there is no diminution in the observed rate constant in the presence of added tri-n-butyltin hydride (entry 6, Table 1), we conclude that the substitution reaction proceeds via a thermal process devoid of radical-chain character. The possible inhibitory effect of CO on the reaction rate was also investigated. Entry 7 (Table 1) reveals that the pseudo-first-order rate constant is essentially unaffected in the presence of 1 atm of CO. This independence of k_{obsd} in the presence of CO provides valuable insight concerning the nature of the observed ligand-independent (k_1) process (vide infra).

The reaction of Ph_2PH with $Co_4(CO)_9(\mu_4\text{-PPh})_2(Ph_2PH)$ (eq. 2) followed pseudo-first-order kinetics for a minimum of three half-lives over the temperature range between 26 and 56°C. Figure 3 shows the infrared spectral changes that accompany the formation of the bis-substituted cluster $Co_4(CO)_8(\mu_4\text{-PPh})_2(Ph_2PH)_2$ (**3**). Further reaction of **3** with Ph_2PH is negligible as the isosbestic points at 2045, 2032, 2009, 2002, 1989 and 1845 cm^{-1} are maintained throughout the course of the reaction. Table 3 lists the obtained pseudo-first-order rate constants k_{obsd} while Fig. 4 reveals the linear relationship between k_{obsd} and the phosphine concentration. The intercepts and slopes afford the ligand-independent and ligand-dependent rate constants k_1 and k_2, respectively, and are listed in Table

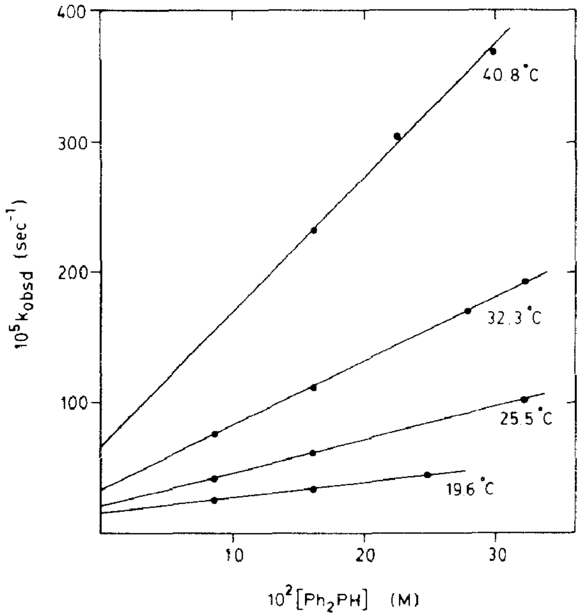

Fig. 2. Plot of k_{obsd} vs. Ph_2PH concentration for the reaction of $Co_4(CO)_{10}(\mu_4\text{-}PPh)_2$ (1) with Ph_2PH at various temperatures, as indicated.

4. As in the mono-substitution step, there is no major rate retardation in the presence of added tri-n-butyltin hydride (entry 6, Table 3) which is the result expected for a purely thermal substitution reaction that lacks a radical-chain

Table 1

Experimental rate constants for the reaction of $Co_4(CO)_{10}(\mu_4\text{-}PPh)_2$ (1) with Ph_2PH [a]

Entry no.	Temperature (°C)	$10^2[Ph_2PH]$ (M)	$10^5\ k_{obsd}$ [b] (s^{-1})
1	19.6	8.6	25 ± 1
2	19.6	16.1	34 ± 1
3	19.6	24.7	45 ± 2
4	25.5	8.6	42 ± 1
5	25.5	16.1	62 ± 2
6	25.5	16.1 [c]	68 ± 1
7	25.5	16.1 [d]	68 ± 1
8	25.5	32.2	102 ± 3
9	32.3	8.6	77 ± 2
10	32.3	16.1	113 ± 2
11	32.3	28.0	171 ± 5
12	32.3	32.2	195 ± 8
13	40.8	16.1	234 ± 8
14	40.8	22.6	306 ± 4
15	40.8	29.0	369 ± 12

[a] From 8.2×10^{-3} M $Co_4(CO)_{10}(\mu_4\text{-}PPh)_2$ in toluene by following the disappearance of the 2040 cm^{-1} IR band. All kinetic data quoted represent single experimental runs that have been appropriately rounded off. [b] Error limits at 95% confidence limit. [c] In the presence of 0.04 M tri-n-butyltin hydride. [d] In the presence of 1 atm of CO.

Table 2

Ligand-independent and ligand-dependent rate constants for the ligand substitution of $Co_4(CO)_{10}(\mu_4\text{-}PPh)_2$ (**1**) with Ph_2PH [a]

Temperature (°C)	$10^5\ k_1$ (s^{-1})	$10^5\ k_2$ ($M^{-1}\ s^{-1}$)
19.6	15.1 ± 0.3	120 ± 2
25.5	21 ± 2	252 ± 10
32.3	34 ± 5	494 ± 21
40.8	65 ± 26	1050 ± 111

[a] From Fig. 1. Error limits at the 95% confidence level.

component.

$$\underset{(2)}{Co_4(CO)_9(\mu_4\text{-}PPh)_2(Ph_2PH)} + Ph_2PH \rightarrow \underset{(3)}{Co_4(CO)_8(\mu_4\text{-}PPh)_2(Ph_2PH)_2} + CO \quad (2)$$

X-ray structure of $Co_4(CO)_8(\mu_4\text{-}PPh)_2(Ph_2PH)_2$

Single-crystal X-ray diffraction analysis was employed in order to determine the regiochemical and stereochemical disposition of the two ancillary Ph_2PH groups in $Co_4(CO)_8(\mu_4\text{-}PPh)_2(Ph_2PH)_2$. Previous examples of bis-substituted clusters of the

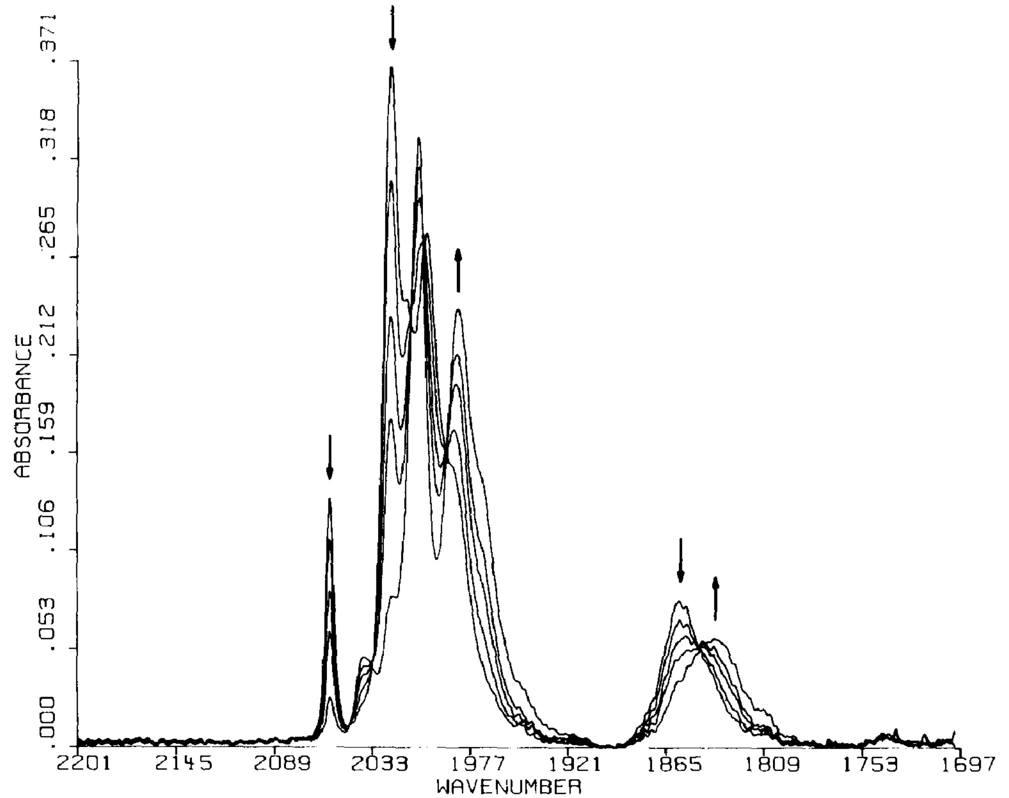

Fig. 3. Typical infrared spectral changes accompanying the ligand substitution of $Co_4(CO)_9(\mu_4\text{-}PPh)_2(Ph_2PH)$ (**2**) with Ph_2PH to afford $Co_4(CO)_8(\mu_4\text{-}PPh)_2(Ph_2PH)_2$ (**3**).

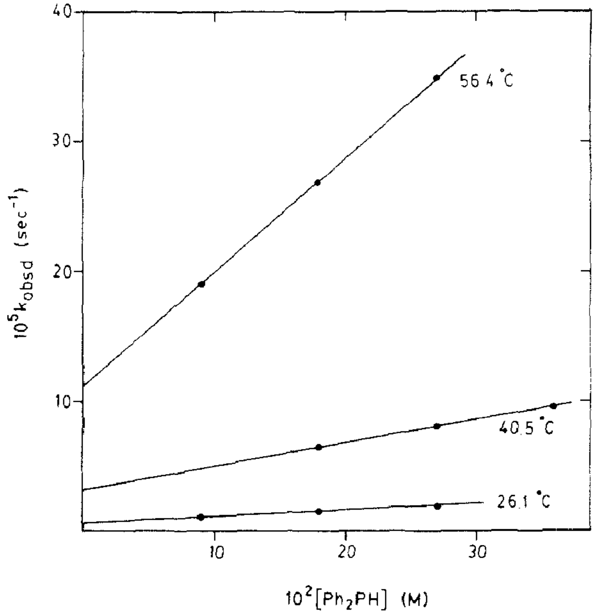

Fig. 4. Plot of k_{obsd} vs. Ph_2PH concentration for the reaction of $Co_4(CO)_9(\mu_4\text{-}PPh)_2(Ph_2PH)$ (**2**) with Ph_2PH at various temperatures, as indicated.

Table 3

Experimental rate constants for the reaction of $Co_4(CO)_9(\mu_4\text{-}PPh)_2(Ph_2PH)$ (**2**) with Ph_2PH [a]

Entry no.	Temperature (°C)	$10^2[Ph_2PH]$ (M)	$10^5\ k_{obsd}$ [b] (s^{-1})
1	26.1	9.0	1.0 ± 0.03
2	26.1	18.0	1.5 ± 0.1
3	26.1	27.0	1.9 ± 0.1
4	40.5	18.0	6.3 ± 0.2
5	40.5	27.0	8.1 ± 0.2
6	40.5	27.0 [c]	7.5 ± 0.2
7	40.5	36.0	9.6 ± 0.1
8	56.4	9.0	19 ± 1
9	56.4	18.0	27 ± 1
10	56.4	27.0	35 ± 1

[a] From 8.2×10^{-3} M $Co_4(CO)_9(\mu_4\text{-}PPh)_2(Ph_2PH)$ in toluene by following the disappearance of the 2058 cm^{-1} IR band. All kinetic data quoted represent single experimental runs that have been appropriately rounded off. [b] Error limits at 95% confidence level. [c] In the presence of 0.04 M tri-n-butyltin hydride.

Table 4

Ligand-independent and ligand-dependent rate constants for the ligand substitution of $Co_4(CO)_9(\mu_4\text{-}PPh)_2(Ph_2PH)$ (**2**) with Ph_2PH [a]

Temperature (°C)	$10^5\ k_1$ (s^{-1})	$10^5\ k_2$ (M^{-1} s^{-1})
26.1	0.6 ± 0.1	5.0 ± 0.4
40.5	3.1 ± 0.6	18 ± 2
56.4	11.2 ± 0.1	88 ± 0.3

[a] From Fig. 4. Error limits at the 95% confidence level.

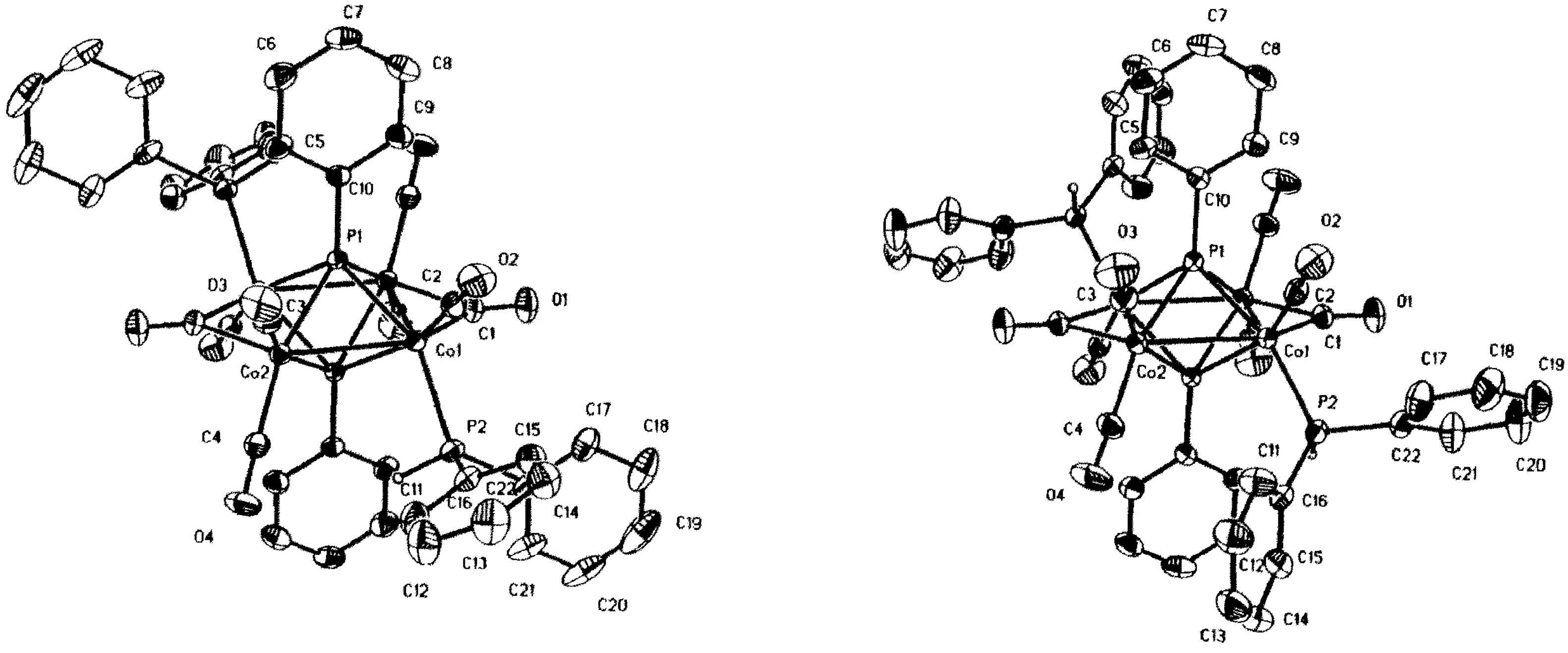

molecule A

molecule B

Fig. 5. ORTEP diagrams of the independent molecules of $Co_4(CO)_8(\mu_4\text{-}PPh)_2(Ph_2PH)_2$ (3) with thermal ellipsoids drawn at the 25% probability level. For clarity, the hydrogen atoms associated with the aryl rings are not included.

form $Co_4(CO)_8(\mu_4\text{-}PPh)_2L_2$ (where L = monodentate ligand) reveal diverse structures. For example, with the small cone angle ligands $P(OMe)_3$ [53] and $P(OEt)_3$ [51] (cone angle of 107° and 109°, respectively [58,59*]) the phosphites are observed to adopt a 1,3-*trans* configuration about the cluster polyhedron while use of the larger phosphine PPh_3 (cone angle 145°) leads to a 1,3-*cis*-phosphine arrangement [54]. Crystals of **3** were observed to contain two fully independent molecules in the unit cell that are structurally similar; the major difference being the disposition of the aryl groups associated with the Ph_2PH ligands. The X-ray data collection and processing parameters for **3** are given in Table 5 with the final fractional coordinates listed in Table 6.

The ORTEP diagram in Fig. 5 shows the molecular structure of **3** and establishes the 1,3-*trans* orientation of the two Ph_2PH ligands. Selected bond distances and angles are given in Tables 7 and 8, respectively. The cobalt atoms in each molecule are planar and form a rectangular array which is capped by a pair of μ_4-phenylphosphinidene groups giving rise to an octahedral $Co_4(\mu_4\text{-}P)_2$ core typical of this genre of cluster [41,51–55,60]. Each cobalt atom is seven-coordinate and the geometry is probably best described as a distorted capped octahedron. The Co–Co, Co–CO, and Co–P(μ_4) bond lengths and angles are unexceptional in comparison to the parent cluster $Co_4(CO)_{10}(\mu_4\text{-}PPh)_2$ [60] and the reported bis-phosphite clusters [51,55] and will not be discussed further.

The Co–Ph_2PH distance of 2.209(9) Å (ave) is in agreement with other cobalt–phosphine distances reported [41b,52,54]. The capping phenyl groups are planar (0.004 Å rmsd. for molecules A and B) and are essentially perpendicular,

Table 5

X-ray crystallographic collection and processing data for $Co_4(CO)_8(\mu_4\text{-}PPh)_2(Ph_2PH)_2$ (**3**)

Space group	$P\bar{1}$
Cell constants	
a, Å	9.800(1)
b, Å	14.849(2)
c, Å	15.583(2)
α, Å	83.89(1)
β, Å	81.69(1)
γ, Å	79.34(1)
V, Å^3	2197.7(5)
Molecular formula	$C_{44}H_{32}Co_4P_4O_8$
fw	1048.32
Formula units per cell (Z)	2
ρ, g cm^{-1}	1.584
Abs. coeff. (μ), cm^{-1}	16.76
Radiation (λ), Å	0.71073
Collection range, deg	$3.0° \leq 2\theta \leq 45.0°$
Total data collected	5744
Independent data, $I > 3\sigma(I)$	4860
Total variables	542
R	0.0379
R_w	0.0414
Weights	$w = [\sigma^2(F_o) + 0.00025F_o^2]^{-1}$

Table 6

Positional parameters for non-hydrogen atoms for $Co_4(CO)_8(\mu_4\text{-PPh})_2(Ph_2PH)_2$ (3) with estimated standard deviations in parentheses

	x	*y*	*z*	U^a
Co(1A)	4445(1)	1009(1)	650(1)	34(1)
Co(2A)	6852(1)	−166(1)	205(1)	35(1)
C(1A)	2539(5)	1300(3)	453(3)	44(2)
O(1A)	1495(4)	1784(3)	589(2)	72(2)
C(2A)	4335(5)	979(3)	1801(3)	49(2)
O(2A)	4331(4)	947(3)	2529(2)	82(2)
C(3A)	7513(5)	−565(3)	1209(3)	47(2)
O(3A)	7944(4)	−752(3)	1855(2)	80(2)
C(4A)	8197(5)	451(3)	−297(3)	48(2)
O(4A)	9057(4)	851(3)	−586(3)	78(2)
P(1A)	4724(1)	−525(1)	666(1)	32(1)
C(5A)	5272(5)	−2055(3)	1826(3)	49(2)
C(6A)	4964(6)	−2629(3)	2568(3)	63(2)
C(7A)	3756(6)	−2404(4)	3110(3)	65(2)
C(8A)	2835(6)	−1621(4)	2921(3)	65(2)
C(9A)	3133(5)	−1061(3)	2181(3)	52(2)
C(10A)	4359(4)	−1268(3)	1629(3)	37(1)
P(2A)	5169(1)	2350(1)	365(1)	42(1)
C(11A)	7566(5)	2467(4)	1090(4)	65(2)
C(12A)	8285(6)	2654(4)	1727(4)	85(3)
C(13A)	7566(7)	2984(4)	2482(4)	84(3)
C(14A)	6166(6)	3145(4)	2595(3)	68(2)
C(15A)	5429(5)	2969(3)	1965(3)	57(2)
C(16A)	6125(5)	2629(3)	1202(3)	45(2)
C(17A)	2719(6)	3617(3)	656(4)	71(2)
C(18A)	1836(7)	4461(4)	540(4)	97(3)
C(19A)	2239(10)	5079(4)	−102(6)	114(4)
C(20A)	3470(9)	4909(4)	−628(5)	97(4)
C(21A)	4364(7)	4070(3)	−505(4)	73(2)
C(22A)	3977(5)	3428(3)	148(3)	52(2)
Co(1B)	47(1)	3914(1)	4514(1)	39(1)
Co(2B)	1925(1)	4955(1)	4782(1)	40(1)
C(1B)	−1903(5)	3874(3)	4707(3)	47(2)
O(1B)	−2732(4)	3440(3)	4616(2)	75(2)
C(2B)	551(5)	3758(3)	3394(4)	55(2)
O(2B)	936(5)	3660(3)	2679(3)	92(2)
C(3B)	2935(5)	5091(3)	3744(3)	56(2)
O(3B)	3614(4)	5123(3)	3086(3)	98(2)
C(4B)	3287(5)	4303(4)	5355(3)	57(2)
O(4B)	4201(4)	3916(3)	5684(3)	101(2)
P(1B)	−151(1)	5448(1)	4266(1)	37(1)
C(5B)	585(5)	6623(3)	2832(3)	59(2)
C(6B)	492(6)	7041(4)	2002(4)	81(3)
C(7B)	−460(7)	6845(4)	1515(4)	83(3)
C(8B)	−1310(6)	6225(4)	1846(3)	72(2)
C(9B)	−1231(5)	5805(3)	2685(3)	57(2)
C(10B)	−288(4)	6004(3)	3177(3)	44(2)
P(2B)	628(1)	2469(1)	5001(1)	47(1)
C(11B)	3520(6)	2127(4)	4561(4)	79(2)
C(12B)	4861(6)	1709(4)	4680(4)	92(3)
C(13B)	5093(7)	1168(4)	5421(4)	91(3)
C(14B)	4048(7)	1060(4)	6062(5)	92(3)

Table 6 (continued)

	x	y	z	U^a
C(15B)	2688(6)	1488(4)	5949(4)	74(2)
C(16B)	2409(5)	2005(3)	5189(3)	53(2)
C(17B)	918(7)	1495(4)	3530(4)	86(3)
C(18B)	528(8)	932(4)	3009(4)	102(3)
C(19B)	−576(8)	500(4)	3280(5)	99(3)
C(20B)	−1325(7)	664(5)	4051(5)	109(4)
C(21B)	−941(6)	1228(4)	4589(4)	84(3)
C(22B)	189(5)	1652(3)	4338(3)	54(2)

[a] Equivalent isotropic U defined as one third of the trace of the orthogonalised U_{ij} tensor.

89.6(7)° and 85.5(7)°, to the plane of the cobalt atoms. These same capping phenyl groups in each molecule are also coplanar. The P(2)Co(1)C(2)O(2) groups are planar (0.01 and 0.02 Å rmsd. in A and B, respectively) and make angles of 88.4(7)° and 81.5(7)° with the cobalt planes. The main difference between the two independent molecules is a rotation around the Co(1)–P2 bond of about 58°.

Discussion

The rate law that best describes our kinetic data for Ph_2PH substitution in $Co_4(CO)_{10}(\mu_4\text{-}PPh)_2$ (**1**) and $Co_4(CO)_9(\mu_4\text{-}PPh)_2(Ph_2PH)$ (**2**) consists of a phosphine-independent first-order and phosphine-dependent second-order contribution, i.e.:

$$\text{rate} = k_{\text{obsd}}[\text{cluster}] = (k_1 + k_2[Ph_2PH])[\text{cluster}] \tag{3}$$

Table 7

Selected bond distances (Å) in the two independent molecules of $Co_4(CO)_8(\mu_4\text{-}PPh)_2(Ph_2PH)_2$ (**3**) [a]

Co(1A)–Co(2A)	2.711(1)	Co(1A)–C(1A)	1.900(5)
Co(1A)–C(2A)	1.777(4)	Co(1A)–P(1A)	2.241(1)
Co(1A)–P(2A)	2.217(1)	Co(1A)–Co(2A′)	2.526(1)
Co(1A)–P(1A′)	2.235(1)	Co(2A)–C(3A)	1.761(5)
Co(2A)–C(4A)	1.785(5)	Co(2A)–P(1A)	2.246(1)
Co(2A)–C(1A′)	2.015(5)	C(1A)–O(1A)	1.142(5)
Co(2A)–P(1A′)	2.238(1)	C(2A)–O(2A)	1.130(5)
C(3A)–O(3A)	1.135(6)	C(4A)–O(4A)	1.134(6)
P(1A)–C(10A)	1.800(4)	P(1A) ··· P(1A′)	2.518(2)
P(2A)–C(16A)	1.833(5)	P(2A)–C(22A)	1.830(4)
Co(1B)–Co(2B)	2.712(1)	Co(1B)–C(1B)	1.903(5)
Co(1B)–C(2B)	1.770(5)	Co(1B)–P(1B)	2.247(1)
Co(1B)–P(2B)	2.200(1)	Co(1B)–Co(2B′)	2.517(1)
Co(1B)–P(1B′)	2.232(1)	Co(2B)–C(3B)	1.782(5)
Co(2B)–C(4B)	1.789(5)	Co(2B)–P(1B)	2.262(1)
Co(2B)–C(1B′)	1.982(5)	C(1B)–O(1B)	1.158(7)
Co(2B)–P(1B′)	2.244(1)	C(2B)–O(2B)	1.138(7)
C(3B)–O(3B)	1.140(6)	C(4B)–O(4B)	1.129(6)
P(1B)–C(10B)	1.818(4)	P(1B) ··· P(1B′)	2.548(2)

[a] A and B refer to the two independent molecules while ′ indicates an atom related by the center symmetry.

Table 8

Selected angles (°) in the two independent molecules of $Co_4(CO)_8(\mu_4\text{-}PPh)_2(Ph_2PH)_2$ (**3**) [a]

Co(2A)–Co(1A)–C(1A)	141.9(1)	Co(2A)–Co(1A)–C(2A)	103.3(1)
C(1A)–Co(1A)–C(2A)	102.9(2)	Co(2A)–Co(1A)–P(1A)	52.9(1)
C(1A)–Co(1A)–P(1A)	98.7(1)	C(2A)–Co(1A)–P(1A)	92.9(1)
Co(2A)–Co(1A)–P(2A)	101.0(1)	C(1A)–Co(1A)–P(2A)	103.1(1)
C(2A)–Co(1A)–P(2A)	96.4(2)	P(1A)–Co(1A)–P(2A)	153.7(1)
Co(2A)–Co(1A)–Co(2A′)	90.1(1)	C(1A)–Co(1A)–Co(2A′)	51.8(1)
C(2A)–Co(1A)–Co(2A′)	126.9(2)	P(1A)–Co(1A)–Co(2A′)	55.6(1)
P(2A)–Co(1A)–Co(2A′)	131.5(1)	Co(2A)–Co(1A)–P(1A′)	52.7(1)
C(1A)–Co(1A)–P(1A′)	96.0(1)	C(2A)–Co(1A)–P(1A′)	155.3(1)
P(1A)–Co(1A)–P(1A′)	68.5(1)	P(2A)–Co(1A)–P(1A′)	94.6(1)
Co(2A′)–Co(1A)–P(1A′)	55.9(1)	Co(1A)–Co(2A)–C(3A)	104.8(1)
Co(1A)–Co(2A)–C(4A)	110.6(1)	C(3A)–Co(2A)–C(4A)	99.4(2)
Co(1A)–Co(2A)–P(1A)	52.8(1)	C(3A)–Co(2A)–P(1A)	94.0(2)
C(4A)–Co(2A)–P(1A)	161.2(1)	Co(1A)–Co(2A)–Co(1A′)	89.9(1)
C(3A)–Co(2A)–Co(1A′)	127.0(2)	C(4A)–Co(2A)–Co(1A′)	122.7(2)
P(1A)–Co(2A)–Co(1A′)	55.5(1)	Co(1A)–Co(2A)–C(1A′)	137.6(1)
C(3A)–Co(2A)–C(1A′)	100.6(2)	C(4A)–Co(2A)–C(1A′)	97.8(2)
P(1A)–Co(2A)–C(1A′)	92.5(1)	Co(1A′)–Co(2A)–C(1A′)	47.8(1)
Co(1A)–Co(2A)–P(1A′)	52.6(1)	C(3A)–Co(2A)–P(1A′)	156.7(1)
C(4A)–Co(2A)–P(1A′)	95.0(2)	P(1A)–Co(2A)–P(1A′)	68.3(1)
Co(1A′)–Co(2A)–P(1A′)	55.7(1)	C(1A′)–Co(2A)–P(1A′)	95.4(1)
Co(1A)–C(1A)–O(1A)	146.1(4)	Co(1A)–C(1A)–Co(2A′)	80.3(2)
O(1A)–C(1A)–Co(2A′)	133.5(4)	Co(1A)–C(2A)–O(2A)	176.8(4)
Co(2A)–C(3A)–O(3A)	174.8(5)	Co(2A)–C(4A)–O(4A)	177.5(5)
Co(1A)–P(1A)–Co(2A)	74.3(1)	Co(1A)–P(1A)–C(10A)	123.8(1)
Co(2A)–P(1A)–C(10A)	123.3(1)	Co(1A)–P(1A)–Co(1A′)	111.5(1)
Co(2A)–P(1A)–Co(1A′)	68.6(1)	C(10A)–P(1A)–Co(1A′)	124.6(1)
Co(1A)–P(1A)–Co(2A′)	68.7(1)	Co(2A)–P(1A)–Co(2A′)	111.7(1)
C(10A)–P(1A)–Co(2A′)	125.1(1)	Co(1A′)–P(1A)–Co(2A′)	74.6(1)
Co(1A)–P(1A)–P(1A′)	55.6(1)	Co(2A)–P(1A)–P(1A′)	55.7(1)
C(10A)–P(1A)–P(1A′)	178.8(2)	Co(1C)–P(1A)–P(1A′)	55.9(1)
Co(2C)–P(1A)–P(1A′)	56.0(1)	C(16A)–P(2A)–C(22A)	102.8(2)
Co(2B)–Co(1B)–C(1B)	141.5(1)	Co(2B)–Co(1B)–P(1B)	53.3(1)
C(1B)–Co(1B)–C(2B)	105.0(2)	C(2B)–Co(1B)–P(1B)	91.8(1)
C(1B)–Co(1B)–P(1B)	96.9(1)	C(1B)–Co(1B)–P(2B)	93.2(1)
Co(2B)–Co(1B)–P(2B)	112.2(1)	P(1B)–Co(1B)–P(2B)	164.4(1)
C(2B)–Co(1B)–P(2B)	97.0(1)	C(1B)–Co(1B)–Co(2B′)	51.0(1)
Co(2B)–Co(1B)–Co(2B′)	90.5(1)	P(1B)–Co(1B)–Co(2B′)	55.9(1)
C(2B)–Co(1B)–Co(2B′)	128.8(1)	Co(2B)–Co(1B)–P(1B′)	52.9(1)
P(2B)–Co(1B)–Co(2B′)	124.8(1)	C(2B)–Co(1B)–P(1B′)	152.7(2)
C(1B)–Co(1B)–P(1B′)	97.0(1)	P(2B)–Co(1B)–P(1B′)	97.7(1)
P(1B)–Co(1B)–P(1B′)	69.3(1)	Co(1B)–Co(2B)–C(3B)	104.2(2)
Co(2B′)–Co(1B)–P(1B′)	56.5(1)	C(3B)–Co(2B)–C(4B)	98.1(2)
Co(1B)–Co(2B)–C(4B)	111.8(2)	C(3B)–Co(2B)–P(1B)	94.1(2)
Co(1B)–Co(2B)–P(1B)	52.8(1)	Co(1B)–Co(2B)–Co(1B′)	89.5(1)
C(4B)–Co(2B)–P(1B)	162.7(2)	C(4B)–Co(2B)–Co(1B′)	123.1(2)
C(3B)–Co(2B)–Co(1B′)	128.1(1)	Co(1B)–Co(2B)–C(1B′)	137.7(1)
P(1B)–Co(2B)–Co(1B′)	55.4(1)	C(4B)–Co(2B)–C(1B′)	95.4(2)
C(3B)–Co(2B)–C(1B′)	103.1(2)	Co(1B′)–Co(2B)–C(1B′)	48.2(1)
P(1B)–Co(2B)–C(1B′)	93.7(1)	C(3B)–Co(2B)–P(1B′)	156.3(2)
Co(1B)–Co(2B)–P(1B′)	52.5(1)	P(1B)–Co(2B)–P(1B′)	68.9(1)
C(4B)–Co(2B)–P(1B′)	95.7(2)	C(1B′)–Co(2B)–P(1B′)	94.7(1)
Co(1B′)–Co(2B)–P(1B′)	56.0(1)	Co(1B)–C(1B)–Co(2B′)	80.7(2)
Co(1B)–C(1B)–O(1B)	143.4(4)	Co(1B)–C(2B)–O(2B)	176.9(5)
O(1B)–C(1B)–Co(2B′)	135.8(3)		

Table 8 (continued)

Co(2B)–C(3B)–O(3B)	175.9(4)	Co(2B)–C(4B)–O(4B)	175.9(5)
Co(1B)–P(1B)–Co(2B)	74.0(1)	Co(1B)–P(1B)–C(10B)	120.7(2)
Co(2B)–P(1B)–C(10B)	122.7(1)	Co(1B)–P(1B)–Co(1B′)	110.7(1)
Co(2B)–P(1B)–Co(1B′)	68.1(1)	C(10B)–P(1B)–Co(1B′)	128.6(2)
Co(1B)–P(1B)–Co(2B′)	68.2(1)	Co(2B)–P(1B)–Co(2B′)	111.1(1)
C(10B)–P(1B)–Co(2B′)	125.9(2)	Co(1B′)–P(1B)–Co(2B′)	74.6(1)
Co(1B)–P(1B)–P(1B′)	55.1(1)	Co(2B)–P(1B)–P(1B′)	55.2(1)
C(10B)–P(1B)–P(1B′)	175.2(2)	Co(1B′)–P(1B)–P(1B′)	55.6(1)
Co(2B′)–P(1B)–P(1B′)	55.9(1)	C(16B)–P(2B)–C(22B)	104.0(2)

[a] A and B refer to molecules A and B while ′ indicates an atom related by a center of symmetry.

where the magnitudes of the k_1 and k_2 terms are obtained from the intercepts and slopes, respectively, of Fig. 2 and 4.

Our results reveal that the ligand-dependent process (k_2 term) of each substitution step is dominant, accounting for 96 and 88% of the observed rate at 1.0 *M* Ph_2PH for the conversion of **1** → **2** and **2** → **3**, respectively. Further support for this bimolecular reaction derives from the activation parameters given in Table 9. The moderately low values of $\Delta H^{\neq}$ and negative $\Delta S^{\neq}$ values are consistent with an associative reaction that involves Ph_2PH attack on the cobalt clusters **1** and **2** [61]. Here, as in the earlier report using $P(OMe)_3$ [55], reaction of Ph_2PH with clusters **1** or **2** is believed to lead to an adduct with an expanded cluster polyhedron (Scheme 1). Implicit in this formulation is the required scission of a carbonyl-bridged Co–Co bond coupled with the conversion of the associated μ_2-bridging CO group into a terminal CO group. Application of Polyhedral Skeletal Electron pair (PSEP) theory [62–64*] predicts that the closo clusters **1** and **2** should transform to the corresponding phosphinated nido clusters upon associative Ph_2PH addition [65*,66]. The lifetime of these clusters is anticipated to be short based on the crystallographic results of the related *nido* aminomethylbis(difluorophosphine)-bridged cluster $Co_4(CO)_3(\mu_4\text{-PPh})_2[CH_3N(PF_2)_2]_4$ [67]. There the noncarbonyl-bridged Co–Co bonds and the carbonyl-bridged Co–Co bond are 0.19 and 0.06 Å shorter, respectively, than the corresponding bonds in the *closo* parent cluster **1** [54,60]. Furthermore, the μ_4-P ⋯ μ_4-P nonbonded distance is reduced from 2.540(5) Å in **1** to 2.440(9) Å in $Co_4(CO)_3(\mu_4\text{-PPh})_2[CH_3N(PF_2)_2]_4$ [67] as the "optimum" Co–Co and Co–(μ_4)P distances and angles are perturbed upon adoption of the *nido* polyhedral structure. The observation of *nido*-$Co_4(CO)_3(\mu_4\text{-PPh})_2[CH_3N(PF_2)_2]_4$ is possible due to the bridging nature of $MeN(PF_2)_2$ that promotes the stabilization of novel metal cluster polyhedra [68]. However, use of the monodentate ligand Ph_2PH (as well as others) permits the formation of **2** and **3** upon CO loss and reformation of the Co–Co bond.

The minor unimolecular contribution to the rate law deserves special comment because the current studies provide additional evidence for a structural reorganization of the cluster prior to phosphine capture. The majority of phosphine-independent substitution pathways involving metal clusters typically proceed via dissociative CO loss [6]. However, we feel that this latter manifold is unlikely due to the negative $\Delta S^{\neq}$ values obtained for the conversion of **1** → **2** and **2** → **3** along with a lack of CO inhibition of **1** → **2** (entry 7, Table 1), mandating a CO independent mechanism (Scheme 2). Such an unsaturated intermediate is rather discriminating,

Table 9

Activation parameters for ligand substitution [a]

Substitution	Ligand-independent [b]			Ligand-dependent [b]		
	k_1 [c]	$\Delta H^{\neq}$	$\Delta S^{\neq}$	k_2 [d]	$\Delta H^{\neq}$	$\Delta S^{\neq}$
parent → mono	11.2	12.6 ± 1.1	−33.1 ± 3.7	26.5	18.4 ± 0.9	−8.9 ± 2.9
mono → bis	0.7	19.5 ± 2.5	−17.4 ± 7.9	0.5	18.5 ± 1.6	−16.7 ± 5.1

[a] Error limits at the 95% confidence level. [b] Calculated from the experimental rate data (raw) extrapolated to 50 °C. $\Delta H^{\neq}$ values are in kcal/mol and $\Delta S^{\neq}$ in eu. [c] 10^4 s^{-1}. [d] 10^3 M^{-1} s^{-1}.

reacting with added phosphine in preference to CO [52,55]. In this scheme $k_1 \ll k_{-1}$ and $k_{-1} \ll k_2$ is required for a reversible Co–Co bond scission process independent of saturation kinetics [69,70].

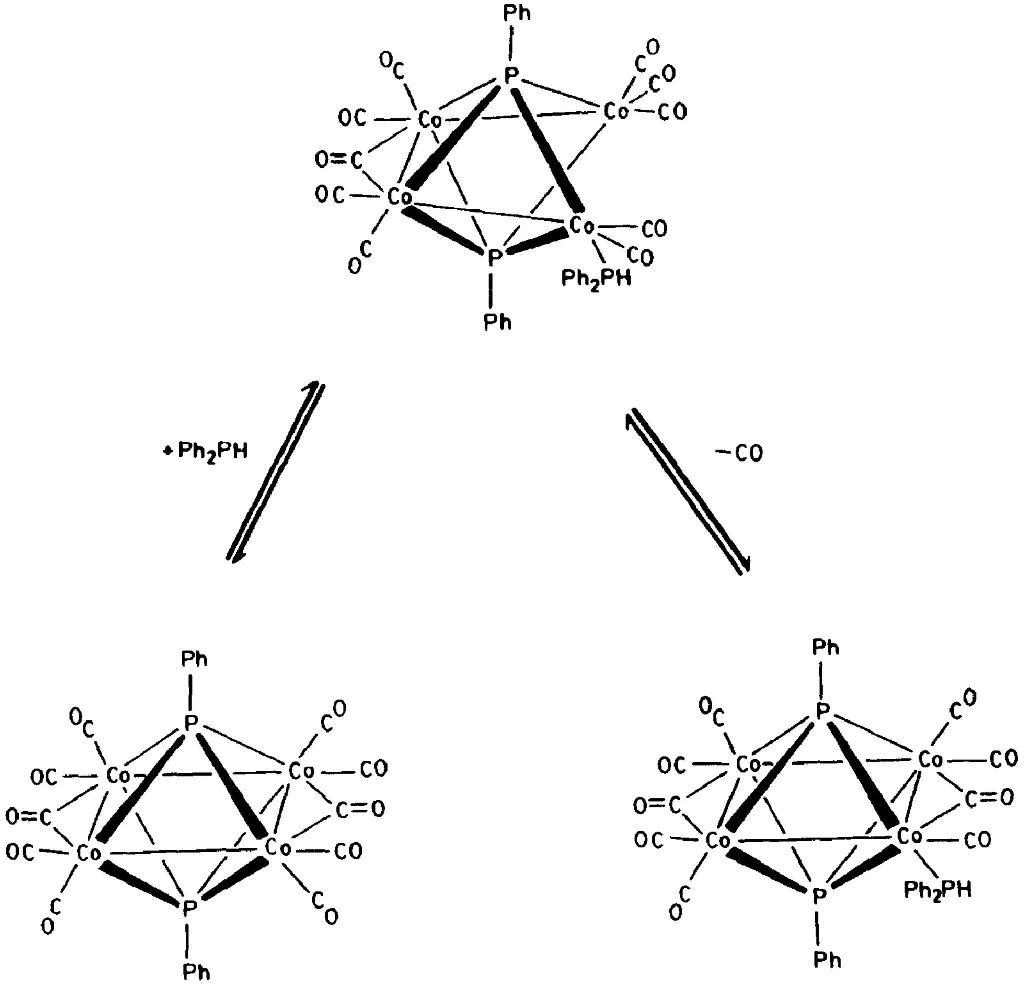

2

Scheme 1

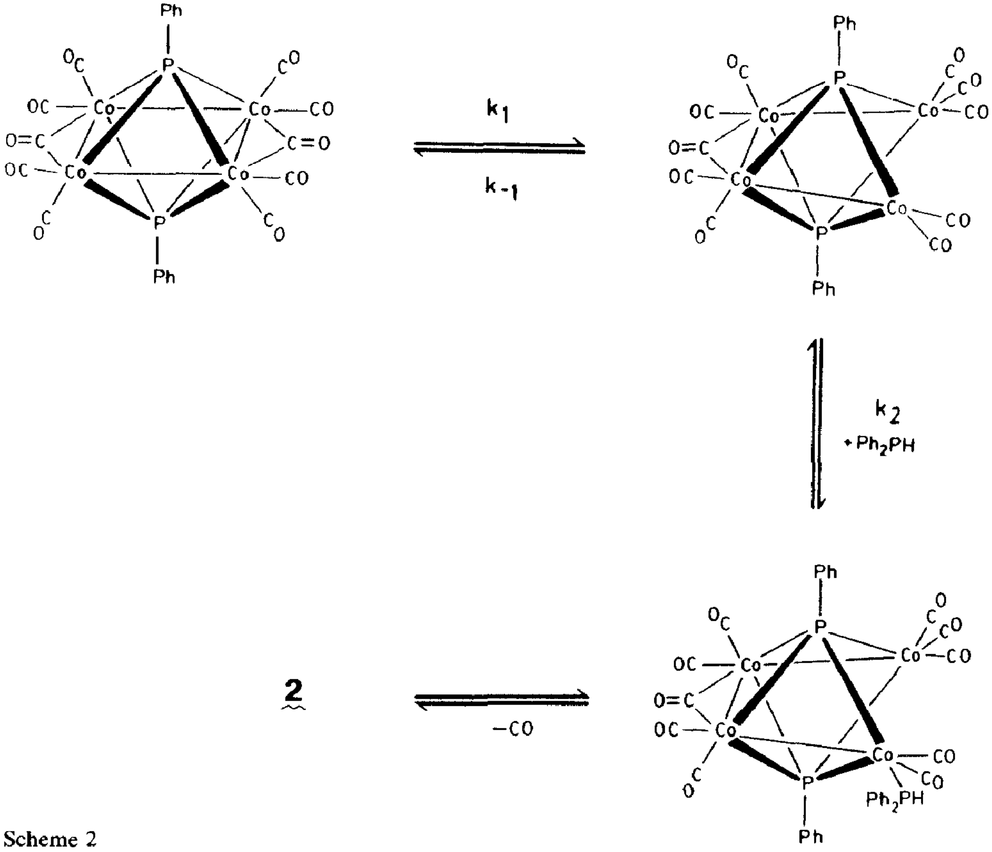

Scheme 2

The rearrangement in Scheme 2 may also be considered as a valence-tautomeric equilibrium which has been unequivocally demonstrated by Huttner and coworkers [40,71*]. However, the observed activation entropies of our systems differ vastly from the tetrahedral clusters examined by Huttner. For example, the reversible scission of the Fe–Mn bond in $Cp(CO)_2MnFe_2(CO)_6(\mu_3\text{-}PPh)$ displays a positive activation entropy ascribed to strain release accompanying the formation of the intermediate edge-opened cluster (cf. a four-vertex *arachno* cluster derived from an octahedron), as shown in Scheme 3.

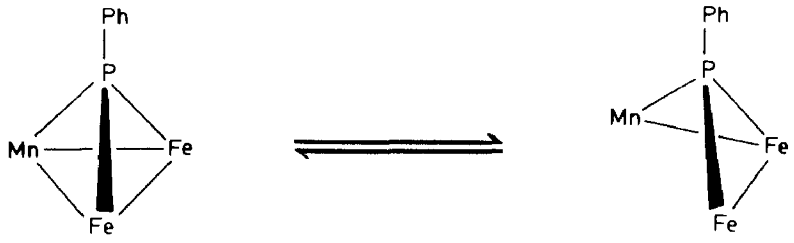

Scheme 3

We believe that an analogous valence tautomerism exists for the tetracobalt clusters **1** and **2**; however, with two μ_4-phenylphosphinidene groups present it is not immediately clear that positive $\Delta S^{\neq}$ values should be expected [72]. Two μ_4-PPh groups are much more confining than the one μ_3-PPh group present in the Huttner clusters. Furthermore, if we consider the Co–Co bond scission in $Co_4(CO)_3(\mu_4$-$PPh)_2[CH_3N(PF_2)_2]_4$ (vide supra) as a rough indicator for the geometrical changes accompanying cluster opening in Scheme 2, we expect severe destabilizing structural perturbations within the cluster core and an overall loss in the degrees of freedom experienced by the cluster. Such a rearrangement should therefore manifest itself in a negative $\Delta S^{\neq}$. Further proof of unimolecular structural reorganizations displaying negative $\Delta S^{\neq}$ values is readily seen in the work of San Fillippo [70], Marks [73], Bryndza and Tam [74], and Carpenter [75]. Additional kinetic studies employing other ligands are clearly required in order to test the substitutional reactivity of the intermediate nido cluster formed via valence tautomerism in **1** and phosphinated derivatives of **2**.

The observed phosphine disposition in **3** represents another example of thermodynamic product control in substitution of **1** with small cone angle, monodentate ligands. Introduction of the first Ph_2PH ligand into **1** yields **2** with no apparent destabilizing interactions. Particularly important at this stage of substitution is the orientation of the phosphinidene phenyl group *cis* to the ancillary P-ligand. If the P-ligand is large, as in the case of PPh_3, severe intramolecular contacts between μ_4-PPh and PPh_3 result causing the phosphinidene phenyl group to twist away from its preferred bisection of the carbonyl-bridged Co–Co bonds [54]. Elongation of the noncarbonyl-bridged Co–Co bond adjacent to the PPh_3 group is also expected [41b,52]. Unfortunately, the mono-substituted cluster $Co_4(CO)_9(\mu_4$-$PPh)_2(PPh_3)$ has not been structurally characterized, but we note that the analogous cluster $Co_4(CO)_9(\mu_4$-$PPh)_2(PCy_3)$ (where Cy = cyclohexyl) bears out these predictions concerning cluster destabilization [76]. In the case of PPh_3, the second incoming ligand is then directed to the opposite cobalt atom to yield the observed 1,3-*cis*-PPh_3 disposition [54]. Adoption of this stereochemistry arises from the fact that 1,3-*trans* stereochemistry would necessitate an unfavorable twisting of both phenylphosphinidene groups.

In the case of Ph_2PH (and other ligands with cone angles less than 128°) we propose that the phosphinidene phenyl group *cis* to Ph_2PH in $Co_4(CO)_9(\mu_4$-$PPh)_2(Ph_2PH)$ experiences no unfavorable, close intramolecular contacts and, thus, does not undergo a destabilizing 90° phenyl twist. Further reaction with a second Ph_2PH ligand leads to 1,3-substitution which may initially involve *cis* or *trans* stereochemistry (1,2-substitution is considered unlikely due to extreme intramolecular $Ph_2PH \cdots Ph_2PH$ and Ph_2PH-cluster crowding). The kinetic stereochemistry is immaterial because carbonyl fluxionality about the cluster polyhedron is rapid ($\sim 10^3$–10^4 s^{-1}) [55] and this serves to assist in the ultimate production of the thermodynamically more stable 1,3-*trans* derivative.

Substitution reactions with other bicapped clusters are planned as part of our interest in cooperative polynuclear interactions and metal-cluster valence-tautomerism. This latter unique reactivity mode underscores the potential of polynuclear clusters to activate substrates through the intrinsic unsaturation associated with metal–metal bonds.

Experimental

General

Dicobalt octacarbonyl and dichlorophenylphosphine were purchased from Pressure Chemical Co. and used as received. $Co_4(CO)_{10}(\mu_4\text{-PPh})_2$ [41], Bu_3SnH [77], and Ph_2PH [78] were all prepared from known literature procedures. All reactions were conducted under argon using Schlenk techniques [79]. Toluene and THF were distilled from sodium/benzophenone ketyl and stored under argon in Schlenk vessels. Infrared spectra were recorded on a Nicolet 20SXB FT-IR spectrometer in 0.1 mm NaCl cells. C and H analyses were performed by Atlantic Microlab, Atlanta, GA.

Synthesis of $Co_4(CO)_9(\mu_4\text{-PPh})_2(Ph_2PH)$ (2)

To 0.5 g (0.68 mmol) of $Co_4(CO)_{10}(\mu_4\text{-PPh})_2$ in 50 ml of toluene was added ~ 0.19 ml (1.0 mmol) of Ph_2PH. The solution was stirred for 2 days at room temperature, after which TLC examination (benzene/petroleum ether, 8/2) revealed ~ 70% conversion to the mono-substituted cluster $Co_4(CO)_9(\mu\text{-PPh})_2(Ph_2PH)$ (**2**). Chromatography over silica gel (benzene/petroleum ether, 8/2) afforded **2** which was recrystallized from toluene/heptane (1/1) at −20 °C to give 0.31 g (yield: 51.2%) of red $Co_4(CO)_9(\mu_4\text{-PPh})_2(Ph_2PH)$. IR (cyclohexane): 2058(m), 2023(vs), 2015(s), 2006(s), 1995(m), 1873(m), and 1862(m) cm^{-1}. Anal. Found: C, 44.63; H, 2.40. $C_{33}H_{21}Co_4O_9P_3$ calcd.: C, 44.51; H, 2.36%.

Synthesis of $Co_4(CO)_8(\mu_4\text{-PPh})_2(Ph_2PH)_2$ (3)

To 0.2 g (0.27 mmol) of $Co_4(CO)_{10}(\mu_4\text{-PPh})_2$ in 40 ml of toluene was added 0.25 ml (1.4 mmol) of Ph_2PH. The solution was stirred for 2 days at room temperature, after which TLC examination (benzene/petroleum ether, 1/1) revealed ~ 85% conversion to the bis-substituted cluster $Co_4(CO)_8(\mu_4\text{-PPh})_2(Ph_2PH)_2$ (**3**). Chromatography over silica gel (benzene/petroleum ether, 1/1) afforded **3** as a dark brown-black solid. The analytical sample and crystals suitable for X-ray diffraction analysis were obtained upon recrystallization using a 1/1 mixture of toluene/heptane at −25 °C. Yield: 0.13 g (45.4%) of **3**. IR (cyclohexane): 2043(w,b), 2009(vs), 1986(s), 1976(m), and 1851(w,b) cm^{-1}. Anal. Found: C, 51.26; H, 3.25. $C_{44}H_{32}Co_4O_8P_4 \cdot 1/4C_7H_8$ calcd.: C, 51.29; H, 3.20.

X-Ray crystallography

A dark brown-black crystal of dimensions 0.15 × 0.20 × 0.38 mm was mounted on a Nicolet R3M/μ update of a $P2_1$ diffractometer. Cell constants were obtained from a least-squares refinement of 25 reflections in the range $25.20° \leq 2\theta \leq 28.55°$. Laue symmetry $\bar{1}$, no systematic absences and statistics are consistent with the space group $P\bar{1}$. Intensity data in the range $3.0° \leq 2\theta \leq 45.8°$ were collected at 296 K in the κ Scan Mode using a variable scan speed and graphite-monochromated Mo-K_α radiation (λ 0.71073 Å). Two reference reflections [(3 6 $\bar{1}$) and (3 2 5)] were monitored periodically during data collection and showed variations of less than ±3%. Lorentz and polarization corrections and a ψ-scan based empirical absorption correction were applied (transmission factors 0.764–0.931). The structure was solved by direct methods and refined by a block-cascade least-squares technique. All hydrogen atoms were located in the difference map, but were allowed to ride at a fixed distance from the attached carbon atoms with a single fixed isotropic temperature factor. All other atoms were refined anisotropically. Refinement converged at $R = 0.0379$ and $R_w = 0.0414$ for 542 parameters and 4860 reflections.

Kinetic studies

All kinetic reactions were conducted under pseudo-first-order conditions, with Ph_2PH concentrations which were greater than 10 times that of the reactant cluster. The reactions were monitored for a minimum of three half-lives by following the IR absorbance of the highest energy ν(CO) band of the starting cluster. Plots of ln A_T vs. time gave the pseudo-first-order rate constants, k_{obsd}, quoted in Tables 2 and 4. Plots of k_{obsd} vs. the Ph_2PH concentration afforded the ligand-independent and ligand-dependent rate constants k_1 and k_2, respectively. The activation parameters ($\Delta H^{\neq}$ and $\Delta S^{\neq}$) were determine using the Arrhenius equation [80]. Error limits were calculated by using the available least-squares regression program [81].

Supplementary material available

Listings of observed and calculated structure factor amplitudes and tables of anisotropic thermal parameters, and idealized hydrogen parameters. Ordering information will be supplied by the authors upon request.

Acknowledgments

Financial support from the National Science Foundation (CHE8514367-WHW), Robert A. Welch Foundation (B-1039-MGR) and the UNT faculty research program (MGR) is gratefully acknowledgement.

References

1 J.K. Kochi, J. Organomet. Chem., 300 (1986) 139.
2 R. Huq and A. Poe, J. Organomet. Chem., 226 (1982) 277.
3 Z.A. Rahman, L.R. Beanan, L.M. Bavaro, S.P. Modi, J.R. Keister and M.R. Churchill, J. Organomet. Chem., 263 (1984) 75.
4 A. Poe and V.C. Sekhar, Inorg. Chem., 24 (1985) 4376.
5 D. Sonnenberger and J.D. Atwood, J. Am. Chem. Soc., 102 (1980) 3484.
6 J.D. Atwood, M.J. Wovkulich and D.C. Sonnenberger, Acc. Chem. Res., 16 (1983) 350.
7 A. Shojaie and J.D. Atwood, Organometallics, 4 (1985) 187.
8 (a) G.F. Stuntz and J.R. Shapley, Inorg. Chem., 15 (1976) 1994. (b) G.F. Stuntz and J.R. Shapley, J. Organomet. Chem., 213 (1981) 389.
9 E.L. Muetterties, R.R. Burch and A.M. Stolzenberg, Ann. Rev. Phys. Chem., 33 (1982) 89.
10 M.V. Twigg, Inorg. Chim. Acta, 21 (1977) L7.
11 J.R. Fox, W.L. Gladfelter and G.L. Geoffroy, Inorg. Chem., 19 (1980) 2574.
12 K. Dahlinger, F. Falcone and A.J. Poe, Inorg. Chem., 25 (1986) 2654.
13 N. Brodie, A. Poe and V. Sekhar, J. Chem. Soc., Chem. Commun., (1985) 1090.
14 A.J. Poe, C.N. Sampson and R.T. Smith, J. Am. Chem. Soc., 108 (1986) 5459.
15 D.J. Taube, R. van Eldik and P.C. Ford, Organometallics, 6 (1987) 125.
16 B. Ambwani, S. Chawla and A. Poe, Inorg. Chem., 24 (1985) 2635.
17 R. Shojaie and J.D. Atwood, Inorg. Chem., 26 (1987) 2199.
18 D.J. Darensbourg, D.J. Zalewski, A.L. Rheingold and R.L. Durney, Inorg. Chem., 25 (1986) 3281.
19 D.J. Darensbourg and M.J. Incorvia, Inorg. Chem., 20 (1981) 1911.
20 D.J. Darensbourg and D.J. Zalewski, Organometallics, 4 (1985) 92.
21 D.J. Darensbourg, D.J. Zalewski and T. Delord, Organometallics, 3 (1984) 1210.
22 D.C. Sonnenberger and J.D. Atwood, J. Am. Chem. Soc., 104 (1982) 2113.

23 D.C. Sonnenberger and J.D. Atwood, Organometallics, 1 (1982) 694.

24 D.C. Sonnenberger and J.D. Atwood, Inorg. Chem., 20 (1981) 3243.

25 D.J. Darensbourg and B.J. Baldwin-Zuschke, J. Am. Chem. Soc., 104 (1982) 3906.

26 D.J. Darensbourg and B.J. Baldwin-Zuschke, Inorg. Chem., 20 (1981) 3846.

27 K.J. Karel and J.R. Norton, J. Am. Chem. Soc., 96 (1974) 6812.

28 R. Shojaie and J.D. Atwood, Inorg. Chem., 27 (1988) 2558.

29 See also: D.J. Darensbourg, Adv. Organomet. Chem., 21 (1982) 113.

30 B.F.G. Johnson, Inorg. Chim. Acta, 115 (1986) L39.

31 M. Arewgoda, B.H. Robinson and J. Simpson, J. Am. Chem. Soc., 105 (1983) 1893.

32 A.J. Poe, Inorg. Chim. Acta, 129 (1987) L17.

33 (a) H.J. Langenbach, E. Keller and H. Vahrenkamp, Angew. Chem. Int. Ed. Engl., 16 (1977) 188; (b) H.J. Langenbach, E. Keller and H. Vahrenkamp, J. Organomet. Chem., 171 (1979) 259.

34 R.D. Adams and L.W. Yang, J. Am. Chem. Soc., 105 (1983) 235.

35 F. Richter and H. Vahrenkamp, Organometallics, 1 (1982) 756.

36 G. Huttner, J. Schreider, H.D. Muller, G. Mohr, J. von Seyerl and L. Wohlfahrt, Angew. Chem. Int. Ed. Engl., 18 (1979) 76.

37 K. Knoll, G. Huttner, L. Zsolnai, I. Jibril and M. Wasiucionek, J. Organomet. Chem.. 294 (1985) 91.

38 H. Vahrenkamp, Phil. Trans. R. Soc. Lond. A, 308 (1982) 17.

39 R.P. Planalp and H. Vahrenkamp, Organometallics, 6 (1987) 492.

40 J. Schneider, M. Minelli and G. Huttner, J. Organomet. Chem., 294 (1985) 75.

41 (a) M.G. Richmond and J.K. Kochi, Inorg. Chem., 25 (1986) 656. (b) M.G. Richmond and J.K. Kochi, Organometallics, 6 (1987) 254.

42 (a) H.H. Ohst and J.K. Kochi, J. Chem. Soc., Chem. Commun., (1986) 121; (b) H.H. Ohst and J.K. Kochi, J. Am. Chem. Soc., 108 (1986) 2987. (c) H.H. Ohst and J.K. Kochi, Inorg. Chem., 25 (1986) 2066.

43 T.M. Bockman and J.K. Kochi, J. Am. Chem. Soc., 109 (1987) 7725.

44 R.T. Baker, J.C. Calabrese, P.J. Krusic, M.J. Therien and W.C. Trogler, J. Am. Chem. Soc., 110 (1988) 8392.

45 G.J. Bezems, P.H. Reiger and R. Visco, J. Chem. Soc., Chem. Commun., (1981) 265.

46 M.I. Bruce, D.C. Kehoe, J.G. Matisons, B.K. Nicholson, P.H. Reiger and M.L. Williams, J. Chem. Soc., Chem. Commun., (1982) 442.

47 M.I. Bruce, J.G. Matisons, B.K. Nicholson and M.L. Williams, J. Organomet. Chem., 236 (1982) C57.

48 A.J. Downard, B.H. Robinson and J. Simpson, Organometallics, 5 (1986) 1122, 1132, 1140.

49 (a) W.C. Trogler, Int. J. Chem. Kinet., 19 (1987) 1025, and ref. therein; (b) P.M. Zizelman, C. Amatore and J.K. Kochi, J. Am. Chem. Soc., 106 (1984) 3771; (c) J.W. Hershberger, R.J. Klingler and J.K. Kochi, ibid., 104 (1982) 3034; 105 (1983) 61; (d) J.W. Hershberger, C. Amatore and J.K. Kochi, J. Organomet. Chem., 250 (1983) 345.

50 (a) R.C. Ryan, C.U. Pitmann, Jr. and J.P. O'Connor, J. Am. Chem. Soc., 99 (1977) 1986; (b) C.U. Pittman, Jr. and R.C. Ryan, CHEMTECH, (1978) 170; (c) C.U. Pittman, Jr., G.M. Wilemon, W.D. Wilson and R.C. Ryan, Angew. Chem. Int. Ed. Engl., 19 (1980) 478; (d) C.U. Pittman, Jr., M.G. Richmond, G.M. Wilemon and M. Absi-Halabi in J.R. Kosak (Ed.), Cataysis of Organic Reactions, Marcel Dekker, New York, 1984; Chapter 5.

51 M.J. Don, M.G. Richmond, W.H. Watson and A. Nagl, Acta Cryst., C45 (1989) 736.

52 C.L. Schulman, M.G. Richmond, W.H. Watson and A. Nagl, J. Organomet. Chem., 368 (1989) 367.

53 M.G. Richmond and J.K. Kochi, Inorg. Chim. Acta, 126 (1987) 83.

54 R.C. Ryan, C.U. Pittman, Jr., J.P. O'Connor and L.F. Dahl, J. Organomet. Chem., 193 (1980) 247.

55 M.G. Richmond and J.K. Kochi, Inorg. Chem., 25 (1986) 1334.

56 For reviews on ETC catalyzed reactions, see: (a) D. Astruc, Angew. Chem. Int. Ed. Engl., 27 (1988) 643; (b) M. Chanon, Acc. Chem. Res., 20 (1987) 214; (c) M. Chanon and M.L. Tobe, Angew. Chem. Int. Ed. Engl., 21 (1982) 1; (d) J.F. Bunnett, Acc. Chem. Res., 11 (1978) 413; (e) J.M. Saveant, ibid., 13 (1980) 323.

57 (a) B.A. Narayanan, C. Amatore and J.K. Kochi, Organometallics, 6 (1987) 129; 5 (1986) 926; 3 (1984) 802; (b) B.A. Narayanan, C. Amatore, C.P. Casey and J.K. Kochi, J. Am. Chem. Soc., 105 (1983) 6351; (c) See also: C.E. Summer and G.O. Nelson, ibid., 106 (1984) 432.

58 (a) C.A. Tolman, Chem. Rev., 77 (1977) 313; (b) H.C. Clark, Israel J. Chem., 15 (1976/77) 210.

59 For a report of larger cone angles for P(OMe)$_3$ and P(OEt)$_3$, see: L. Stahl and R.D. Ernst, J. Am. Chem. Soc., 109 (1987) 5673.

60 R.C. Ryan and L.F. Dahl, J. Am. Chem. Soc., 97 (1975) 6904.

61 (a) F. Basolo and R.G. Pearson, Mechanisms of Inorganic Reactions, Wiley, New York, 1967; (b) J.D. Atwood, Inorganic and Organometallic Reaction Mechanisms, Brooks/Cole Monterey, CA, 1985.

62 (a) K. Wade, Chem. Br., 11 (1975) 177; (b) K. Wade, Adv. Inorg. Chem. Radiochem., 18 (1976) 1; (c) K. Wade, in B.F.G. Johnson, Transition Metal Clusters, Wiley, New York, 1980, Chapter 3; (d) D.M.P. Mingos, Acc. Chem. Res., 17 (1984) 311; (e) D.M.P. Mingos, Nature (London), Phys. Sci., 236 (1972) 99.

63 Also see: (a) B.K. Teo, Inorg. Chem., 23 (1984) 1251; (b) B.K. Teo, G. Longoni and F.R.K. Chung, ibid., 23 (1984) 1257; (c) B.K. Teo, ibid., 24 (1985) 115; (d) D.M.P. Mingos, ibid., 24 (1985) 114.

64 (a) For extended Hückel studies of $M_4(\mu_4\text{-PR})_2$ clusters, see: J.F. Halet, R. Hoffmann and J.Y. Saillard, Inorg. Chem., 24 (1985) 1695; (b) Also see: H.H. Ohst and J.K. Kochi, Organometallics, 5 (1986) 1359.

65 For a review on reactions and reactivity of clusters possessing open polyhedra, see: M.O. Albers, D.J. Robinson and N.J. Coville, Coord. Chem. Rev., 69 (1986) 127.

66 Also see: (a) G. Bor, H.K. Dietler, P. Pino and A.J. Poe, J. Organomet. Chem., 154 (1978) 301; (b) D.J. Darensbourg and D.J. Zalewski, Inorg. Chem., 23 (1984) 4382; (c) H. Vahrenkamp, Adv. Organomet. Chem., 22 (1983) 169; (d) D.A. Lesch and T.B. Rauchfuss, Organometallics, 1 (1982) 499; (e) R.D. Adams, Polyhedron, 4 (1985) 2003, and ref. therein; (f) W. Hieber and T. Kruck, Chem. Ber., 95 (1962) 2027; (g) L.E. Bogan, D.A. Lesch and T.B. Rauchfuss, J. Organomet. Chem., 250 (1983) 429.

67 M.G. Richmond and J.K. Kochi, Inorg. Chem., 26 (1987) 541.

68 R.B. King, Acc. Chem. Res., 13 (1980) 243.

69 (a) M.J. Wax and R.G. Bergman, J. Am. Chem. Soc., 103 (1981) 7028; (b) J.D. Cotton and H.A. Kimlin, J. Organomet. Chem., 294 (1985) 213; (c) H.E. Brynda and R.G. Bergman, J. Am. Chem. Soc., 101 (1979) 4766.

70 G. Sundararajan and J. San Fillippo, Jr., Organometallics, 4 (1985) 606.

71 For a review of phosphinidene-capped clusters, see: G. Huttner and K. Knoll, Angew. Chem. Int. Ed. Engl., 26 (1987) 743.

72 Also see: R.M. Laine, J. Mol. Catal., 14 (1982) 137.

73 G.W. Grynkewich and T.J. Marks, Inorg. Chem., 15 (1976) 1307.

74 H.E. Bryndza and W. Tam, Chem. Rev., 88 (1988) 1163, and ref. therein.

75 (a) D.W. Whitman and B.K. Carpenter, J. Am. Chem. Soc., 104 (1982) 6473; (b) B.K. Carpenter, ibid., 105 (1983) 1700.

76 M.J. Don, M.G. Richmond, W.H. Watson and A. Nagl, unpublished results.

77 H.G. Kuivila and O.F. Beumel, Jr., J. Am. Chem. Soc., 83 (1961) 1246.

78 V.D. Bianco and S. Doronzo, Inorg. Synth., 13 (1976) 161.

79 D.F. Shriver, The Manipulation of Air-Sensitive Compounds, McGraw-Hill, New York, 1969.

80 W. Drenth and H. Kwart, Kinetics Applied to Organic Reactions, Marcel Dekker, New York, 1980.

81 A.J. Gordon and R.A. Ford, The Chemist's Companion. A Handbook of Practical Data, Techniques, and References, Wiley, New York, 1976.